Profile analysis of differentially expressed long non-coding RNAs in metabolic memory induced by high glucose in human umbilical vein endothelial cells

JINGYA CHENG[1*], ANQI HUANG[1*], JI CHENG[1], XIAOYAN PEI[1], LEI YU[1], GUOXI JIN[1] and ERQIN XU[2]

[1]Department of Endocrinology, The First Affiliated Hospital of Bengbu Medical College, Bengbu, Anhui 233004; [2]Department of Physical Diagnostics, Bengbu Medical College, Bengbu, Anhui 233030, P.R. China

Received October 25, 2022; Accepted March 21, 2023

DOI: 10.3892/etm.2023.11987

Abstract. Numerous long non-coding RNAs (lncRNAs) are dysregulated in the hyperglycemia-induced phenomenon of metabolic memory (MM). In the present study, the significance of these lncRNAs in MM was explored by screening for MM-involved differentially expressed lncRNAs (MMDELs) in human umbilical vein endothelial cells (HUVECs) induced by high glucose. A total of nine HUVEC samples were divided into three groups to mimic conditions of low and high glucose environments, as well as induce the state of metabolic memory. The expression of lncRNAs was profiled using RNA sequencing. Bioinformatic analysis was performed using the Gene Ontology and the Kyoto Encyclopedia of Genes and Genomes databases to explore the parental genes from which the lncRNAs are transcribed and target genes of the MMDELs and generate enrichment datasets. Reverse transcription-quantitative PCR was performed to validate the expression levels of the selected lncRNAs. The present study identified 308 upregulated and 157 downregulated MMDELs, which were enriched in numerous physiologic processes. Key functional enrichment terms included 'cell cycle', 'oocyte meiosis' and 'p53 signaling pathway'. In conclusion, certain MMDELs may regulate the expression level of highly associated mRNAs through various mechanisms and pathways, thereby interfering with several processes, such as the regulation of the cell cycle, and affecting vascular endothelial cell function. Furthermore, the disorders of these lncRNAs can be retained in MM, further investigation into the functions of these lncRNAs may result in novel insights and treatments, which could help control MM in patients with diabetes.

Correspondence to: Professor Guoxi Jin, Department of Endocrinology, The First Affiliated Hospital of Bengbu Medical College, 287 Changhuai Road, Longzihu, Bengbu, Anhui 233004, P.R. China
E-mail: jyzjyz1999@163.com

[*]Contributed equally

Key words: diabetes mellitus, long non-coding RNA, high glucose, metabolic memory, RNA sequencing

Introduction

Diabetes mellitus (DM) can result in cardiomyopathy, kidney failure, retinopathy and other complications of chronic hyperglycemia, severely affecting life quality and expectancy in this patient population (1,2). Hyperglycemia-induced endothelial dysfunction causes diabetes-related micro- and macrovascular complications in patients with long-term DM (3). However, endothelial dysfunction persists if hyperglycemia is not controlled in a timely manner; this phenomenon is known as metabolic memory (MM) (4). MM is an obstacle in the treatment of diabetic complications. Oxidative stress, non-enzymatic glycation of proteins, epigenetic changes and chronic inflammation are the four basic mechanisms playing vital roles in MM (5-9). Epigenetic mechanisms, including those involving non-coding RNAs, histone modifications and DNA methylation, are crucial components in the pathology of diabetic complications (7). The roles of long non-coding RNAs (lncRNAs) in diabetes-associated endothelial dysfunction and the effects of lncRNAs on MM-related mechanisms are currently being investigated (10,11).

lncRNAs, which are long transcripts containing >200 nucleotides, are structurally similar to, but functionally different from mRNAs. By acting as molecular sponges or host genes for microRNAs (miRNAs/miRs), serving as scaffolds for specific protein complexes and guiding histone-modifying complexes, lncRNAs serve key roles in the epigenetic mechanisms mediating numerous physiological and pathological processes (12-14). Several previous studies have indicated that lncRNAs are involved in diabetes-related nephropathy, retinopathy and cardiovascular diseases, and numerous lncRNAs, such as ENST00000600527, NONHSAT037576.2 and NONHSAT135706.2, have been reported to demonstrate abnormal expression in vascular endothelial and smooth muscle cells placed under high glucose (HG) culture conditions (14-17). The functions of lncRNAs in diabetic endothelial dysfunction and MM have been gathering increasing attention. In human retinal endothelial cells, lncRNA antisense non-coding RNA in the INK4 locus is highly expressed under

HG conditions, causing the overexpression of vascular endothelial growth factors (VEGFs), which induces angiogenesis (18). HG-treated retinal endothelial cells express high levels of the lncRNA myocardial infarction associated transcript (MIAT), which functions as a competing endogenous RNA (ceRNA) by absorbing miR-150-5p, thereby weakening the miRNA-mediated inhibition of VEGF expression. Accordingly, knockdown of lncRNA MIAT alleviates microvascular dysfunction *in vivo* (19). HG levels can also upregulate the expression of lncRNA metastasis-associated lung adenocarcinoma transcript 1 (MALAT1) in the retinas of rats with diabetes. Silencing MALAT1 expression ameliorates diabetic-induced retinal vasculopathy and inflammation *in vivo* and endothelial dysfunction *in vitro* (20). Furthermore, lncRNA maternally expressed gene 3 (MEG3) levels are significantly reduced in the retinas of mice with diabetes and in endothelial cells subjected to HG concentrations or oxidative stress. Knockdown of lncRNA MEG3 enhances inflammation and retinal vascular dysfunction, and promotes the proliferation and migration of retinal endothelial cells and endothelial tube formation (21). Overexpression of MEG3 alleviates diabetic retinopathy by reducing the expression of TGF-β1 and VEGFs (22).

Determining which lncRNAs are expressed in MM can help uncover their roles in the molecular mechanisms driving MM and may facilitate the therapeutic use of these lncRNAs in the treatment of patients with MM. Therefore, in the present study, RNA sequencing and bioinformatics analyses were used to identify lncRNAs with upregulated [(up)-MM-involved differentially expressed lncRNAs (MMDELs)] and downregulated expression (down-MMDELs) in MM induced by HG conditions.

Materials and methods

Cell groups and establishment of the MM model. Primary human umbilical vein endothelial cells (HUVECs) were purchased from the China Center for Type Culture Collection and were maintained in Modified Eagle's Medium (Hyclone; Thermo Fisher Scientific, Inc.) supplemented with 10% fetal bovine serum (Gibco; Thermo Fisher Scientific, Inc.), 100 U/ml penicillin (Gibco; Thermo Fisher Scientific, Inc.) and 100 μg/ml streptomycin (Gibco; Thermo Fisher Scientific, Inc.) at 37˚C in a humidified, 5% CO_2 chamber. Cell culture and establishment of the MM model were performed as described previously (16,23). Briefly, HUVEC cells in the low glucose (LG) group were cultured with 5 mM glucose and 20 mM mannitol for 6 days. The cells in the HG group were cultured with 25 mM glucose for 6 days. The cells in the MM group were treated for 3 days using 25 mM glucose, followed by another 3 days of treatment using 5 mM glucose and 20 mM mannitol, to induce the state of MM in these cells.

RNA preparation and sequencing. Total RNA was isolated from HUVECs and purified using TRIzol® (cat. no. 15596026, Invitrogen; Thermo Fisher Scientific, Inc.) according to the manufacturer's instructions, the quantity and quality of the RNA were determined using an Agilent 4200 Bioanalyzer (Thermo, Fisher Scientific, Inc.). The RNA integrity was assessed by electrophoresis with denaturing agarose gels. Libraries were constructed using a VAHTS Total RNA-Seq(H/M/R) Library PrepKit for Illumina (cat. no. NR603-02; Vazyme Biotech Co., Ltd.) according to the manufacturer's protocol, and libraries were identified using a Qubit™ dsDNA HS Assay Kit (cat. no. Q32854; Invitrogen; Thermo Fisher Scientific, Inc.) and Agilent High Sensitivity DNA Kit (cat. no. 5067-4626; Agilent Technologies, Inc.). The qualities of the libraries were assessed using a Qubit® 2.0 Fluorometer (Thermo Fisher Scientific, Inc.) and the concentration of DNA in the libraries was analyzed using an Agilent 2100 bioanalyzer (Agilent Technologies, Inc.). Clusters were generated bycBot (Illumina, Inc.) and the libraries were diluted to 10 pm, then sequencing was performed on the Illumina HiSeq 2500 according to the manufacturer's protocol at Shanghai Ao-Ji Biotechnology Co., Ltd (2x150 bp, paired-end). Details of the experimental procedures and instruments used are described in our previous study (24).

Identification and analysis of the parental genes of MMDELs. FastQC (version 0.11.3; https://www.bioinformatics.babraham.ac.uk/projects/fastqc/) was used to ensure the quality of RNA-sequencing (RNA-seq) reads. The reads were trimmed using seqtk (https://github.com/lh3/seqtk), and then Illumina TruSeq adapter sequences, poor reads and ribosome RNA reads were removed. The trimmed reads were mapped onto the *Homo sapiens* genome (hg38) using Hisat2 (version 2.0.4) (25). StringTie (version 1.3.0) and gffcompare (version 0.9.8) were used to assemble and compile transcripts from the trimmed reads (26,27). These transcripts were then compared with the reference annotation databases NONCODE (version 5, http://v5.noncode.org/introduce.php) and Ensembl (http://grch37.ensembl.org/index.html). EdgeR and Venny were used to screen out the differentially expressed lncRNAs in the HG vs. LG and MM vs. LG groups ($P<0.05$ and fold change >2) (28,29). Non-significant differentially expressed lncRNAs were then filtered through the comparison of HG vs. MM group ($P>0.05$), and the intersection of these differentially expressed lncRNAs was illustrated using a Venn diagram. Gene Ontology (GO) and KEGG (https://www.kegg.jp/) analysis were used to examine the enrichment of parental genes from which the lncRNAs are transcribed and the function of MMDELs using clusterProfiler (version 3.16, https://www.bioconductor.org/packages/release/bioc/html/clusterProfiler.html) (30,31).

Construction of lncRNA-mRNA-co-expression network. The Pearson correlation coefficient (PCC) was calculated for the analysis of the correlation between the expression of lncRNAs and mRNAs. LncRNA-mRNA pairs with PCC >0.9 and $P<0.01$ were selected for the construction of the co-expression network, which was visualized using Cytoscape (version 2.8.3) (32). The node degree indicates the number of directly linked neighbors for each node. GO and pathway analyses were also used to estimate the highly correlated candidate coding genes using clusterProfiler (version 3.16).

Reverse transcription-quantitative PCR (RT-qPCR) validation. To minimize selection bias, 3 upregulated and 3 downregulated MMDELs were randomly selected. The expression level of these six MMDELs was quantified using qPCR on a Roche LightCycler 480 (Roche Applied Science). The sequences of the specific primers used and the lengths

Table I. Sequences of PCR primers used in the present study.

Gene	Primer sequences (5' to 3')	PCR product length (bp)
GAPDH	F: CCTGGTATGACAACGAATTTG R: CAGTGAGGGTCTCTCTCTTCC	131
NONHSAT180590.1	F: TCCATTCAGAGAACAGGCCC R: TGTGTTGAGTGATCTCCCCG	189
NONHSAT175141.1	F: AAACAGGGGTGTCAGGGTTG R: CAAGCCCTGTAGGAAGACGG	154
ENST00000603538	F: GGCTTCCTTCTATCCCGCTC R: CCGGAGTGCAACAAAATCCG	92
ENST00000530490	F: CGGAAACGCCAGAAAAGTCG R: GTCAACTCGGGCCACATGAT	103
ENST00000621248	F: ATGCTCGGAAAAGCCTCTGG R: AGACAGGCCAAAACCCACAA	92
ENST00000537869	F: CTGTTCCCGTCATGAGCCTT R: GCAAGGCCCTGAATGAGCTA	83

of the products are indicated in Table I. After the total RNA was isolated from HUVECs according to the aforementioned method. RT-qPCR was performed according to the manufacturer's protocol using a ABScript II cDNA First-Strand Synthesis Kit (cat. no. RK20400; Abclonal Biotech Co., Ltd.) and qPCR was performed using a ABScript II One Step SYBR Green RT-qPCR Kit (cat. no. RK20404; Abclonal Biotech Co., Ltd.). PCR reactions were implemented using the following temperature protocol: 95˚C for 10 min, followed by 40 cycles of 95˚C for 15 sec and 60˚C for 20 sec. Expression levels of target genes were normalized to that of GAPDH, which used as an internal reference gene. The relative expression of each lncRNA was calculated using the $2^{-\Delta\Delta Cq}$ method (33).

Statistical analysis. SPSS software (version 24.0; IBM Corp.) was used for data analysis, and the results are presented as the mean ± SEM. There were three repeats per group. To analyze the RT-qPCR validation data, sample distribution was examined using Shapiro-Wilk test, and Levene's test was used to analyze the homogeneity of variance. One-way ANOVA analysis was used to test overall statistical significance, followed by the Least Significance Difference test for pairwise comparisons. P<0.05 was considered to indicate a statistically significant difference.

Results

Identification of HG-induced MMDELs. Three samples each of normal HUVECs (LG group), HG-induced HUVECs (HG group) and MM-induced HUVECs (MM group) were analyzed using RNA-seq to characterize the differences in the lncRNA expression levels. In a total of nine samples, 41,484 lncRNAs were identified and of these, 36,387 lncRNAs were shared between the three groups examined in the present study (Fig. 1A). These lncRNAs were widely distributed on all chromosomes, with higher numbers of lncRNAs revealed on chromosomes 1 and 2 (Fig. 1B). LncRNAs are classified into six types: Intergenic, exonic-antisense, exonic-sense, bidirectional, intronic-antisense and intronic-sense (34). The most numerous species of the identified lncRNAs were intergenic, followed by the exonic-sense and exonic-antisense types (Fig. 1C). These findings suggested the potential diversity and complexity of regulatory mechanisms.

Using edgeR analysis and comprehensive filtration, 308 up- and 157 downregulated MMDELs were identified. As presented in Fig. 2A, 308 upregulated MMDELs were screened from the intersection of upregulated lncRNAs in all groups; among them, 1,448 lncRNAs were upregulated in the HG vs. LG group (fold-change >2, P<0.05), 793 lncRNAs were upregulated in the MM vs. LG group (fold-change >2, P<0.05) and 37,320 lncRNAs were non-significantly differentially expressed (MM vs. HG; P>0.05). Similarly, 157 downregulated MMDELs were identified from the intersection of downregulated lncRNAs; among them, 1,732 lncRNAs were downregulated in the HG vs. LG group (fold-change <-2, P<0.05), 814 lncRNAs were downregulated in the MM vs. LG group (fold-change <-2, P<0.05) and 37,320 lncRNAs were non-significantly differentially expressed (MM vs. HG; P>0.05) (Fig. 2B). The MMDEL expression profile was presented in a heatmap (Fig. 2C).

GO and KEGG analyses of parental genes of MMDELs. To understand the characteristics and functions of lncRNAs, it is important to investigate their parental genes. In the present study, 465 MMDELs were identified; the parental genes of these 465 MMDELs were annotated using GO and pathway enrichment analysis.

The top 30 GO terms with the highest enrichment factors identified using GO analysis included ‘positive regulation of telomere maintenance’, ‘positive regulation of protein acetylation’, ‘regulation of DNA recombination’ and ‘interstrand cross-link repair’ in biological process (BP) terms, ‘striated muscle thin filament’, ‘spindle microtubule’ and ‘nuclear

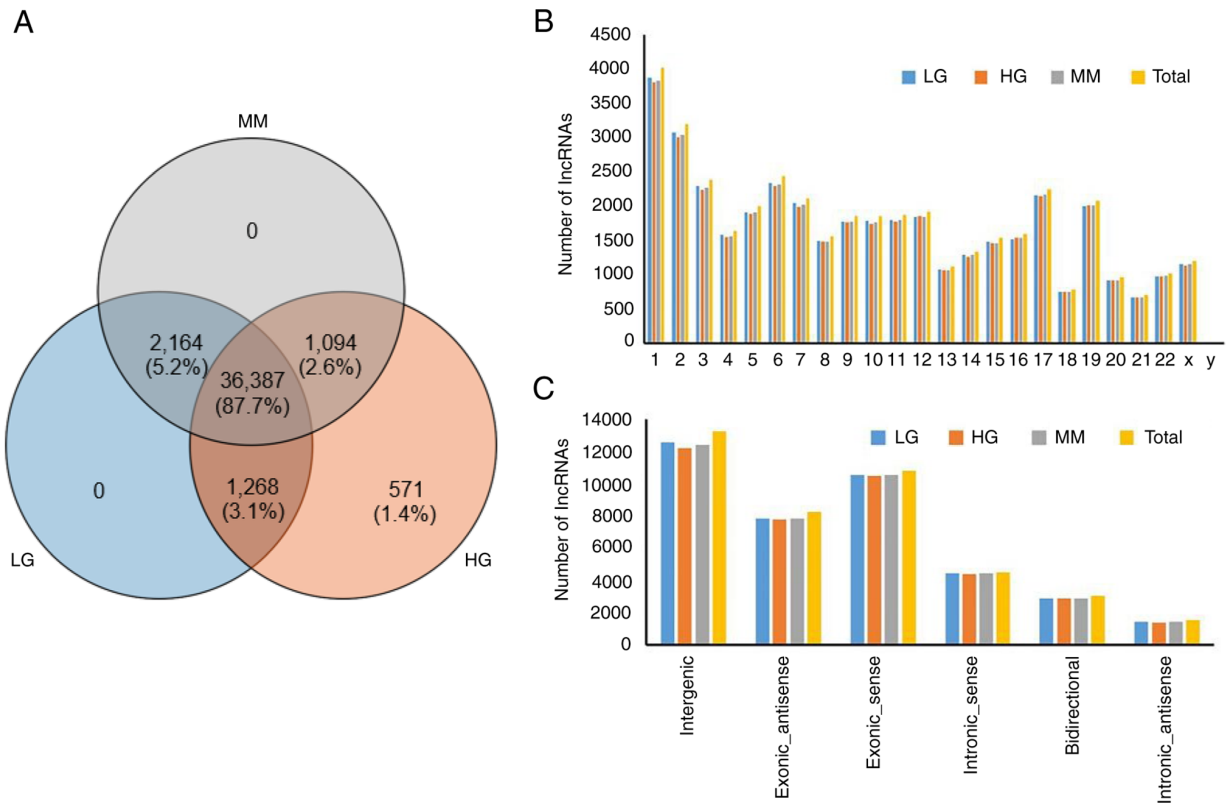

Figure 1. Overview of the lncRNAs identified in all groups examined in the present study. (A) Venn diagram demonstrating the number of lncRNAs mutually expressed in HG, LG and MM groups. (B) Distribution of all lncRNAs identified in the human chromosomes. (C) Number of lncRNAs in each of the six indicated categories. HG, high glucose; LG, low glucose; MM, metabolic memory; lncRNA, long non-coding RNA.

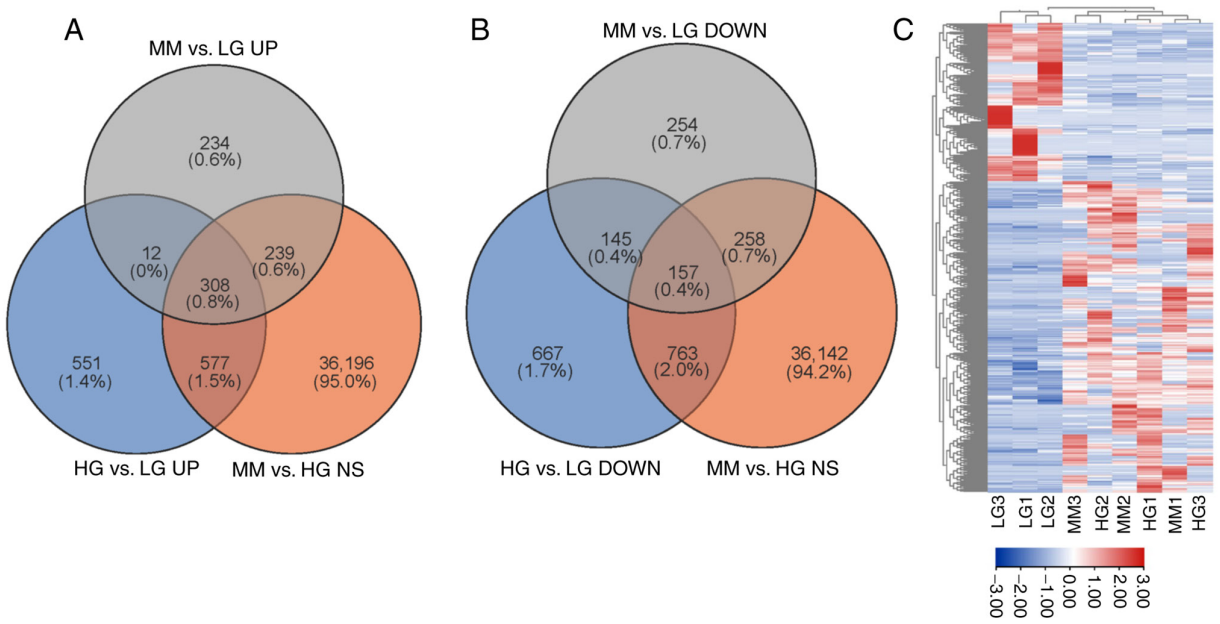

Figure 2. Screening of metabolic-memory related lncRNAs and Venn diagram and heat map of MMDEL. (A) Up-MMDELs and (B) down-MMDELs. HG vs. LG and MM vs. LG comparisons were used to assess upregulated or downregulated expression; the HG vs. MM comparison was used to assess non-significant differential expression. (C) Heatmap indicating all MMDELs assessed in the present study. Red color indicates upregulated and blue color indicates down-regulated expression. HG, high glucose; LG, low glucose; MM, metabolic memory; MMDEL, MM-involved differentially expressed long non-coding RNA; NS, non-significant differential expression.

chromosome, telomeric region' in cellular component (CC) terms, 'NAD binding', 'protein serine/threonine phosphatase activity', 'transcriptional repressor activity, RNA polymerase II transcription factor binding' and 'dioxygenase activity' in molecular function (MF) terms (Fig. 3A). These results indicated disturbances in cell cycle and proliferation.

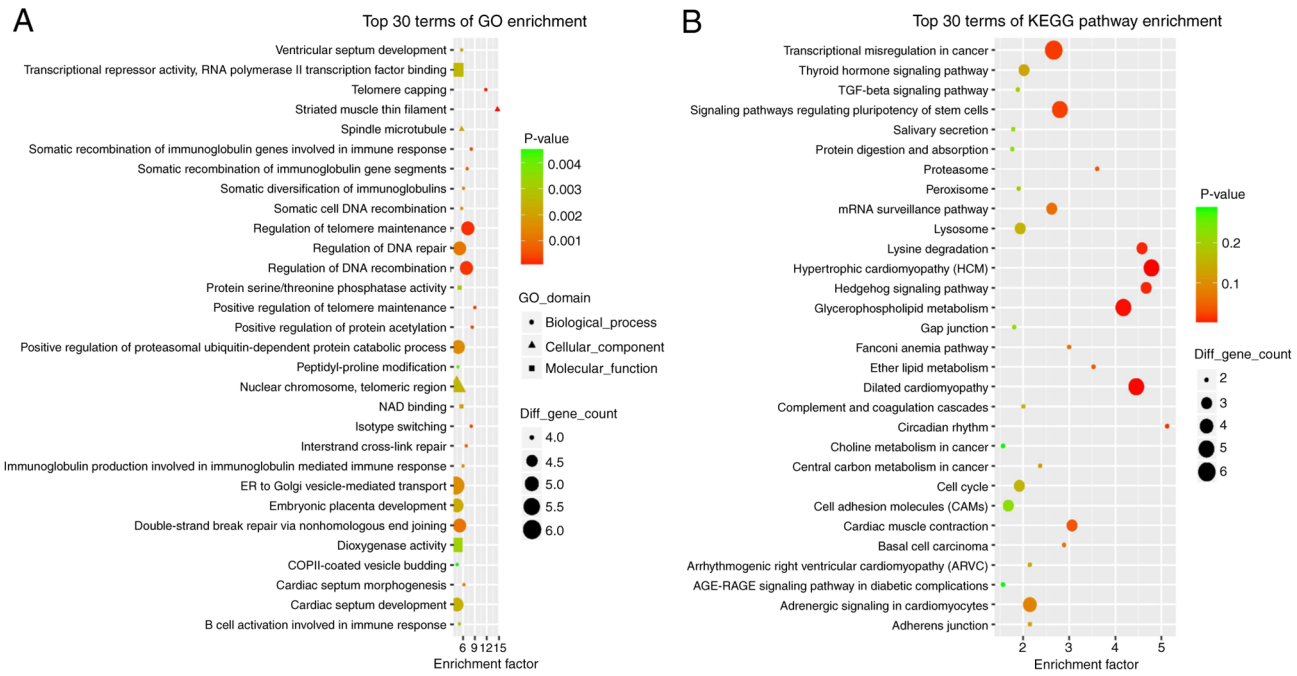

Figure 3. GO and KEGG pathway enrichment analyses of the parental genes of metabolic memory-involved differentially expressed long non-coding RNAs. (A) The top 30 classes of the GO enrichment terms. (B) The top 30 classes of the KEGG pathway enrichment terms. GO, Gene Ontology; KEGG, Kyoto Encyclopedia of Genes and Genomes; Diff_gene_count, differential gene count.

KEGG pathway enrichment analysis indicated that a total of 126 pathway terms were enriched with MMDELs. The top 30 pathways with the highest enrichment factors are demonstrated in Fig. 3B; significantly enriched terms included 'glycerophospholipid metabolism', 'proteasome', 'cardiac muscle contraction', 'signaling pathways regulating pluripotency of stem cells', 'mRNA surveillance pathway', 'cell cycle', 'peroxisome', 'TGF-β signaling pathway' and 'AGE-RAGE signaling pathway in diabetic complications'.

LncRNA-mRNA co-expression network and functional analysis of target mRNAs. To further explore the regulatory role of these lncRNAs, the differentially expressed genes in the same HUVEC samples were evaluated and Cytoscape was used to select the lncRNA-mRNA pairs with PPC (Pearson correlation coefficient) >0.9 and P<0.01 to construct and visualize the co-expression network. Consequently, 397 lncRNA nodes, 708 mRNA nodes and 8,303 edges were used to build the network (Fig. S1). The top 10 up- and downregulated MMDELs with the highest node degree are presented in Table II.

The top 30 GO terms revealed using GO analysis of target mRNAs included 'negative regulation of telomerase activity', 'regulation of double-strand break repair via homologous recombination', 'mitotic cytokinesis', 'negative regulation of DNA biosynthetic process' and 'exit from mitosis' in BP terms, 'condensed nuclear chromosome', 'centromeric region,' 'nuclear nucleosome' and 'mitotic spindle' in CC terms and '14-3-3 protein binding' in MF terms, which were also demonstrated in our previous study (24). This may be attributed to the similar screening criteria used in the two bioinformatics analyses. In this study, we focused on the mRNA whose expression was positively correlated with MMDELs, KEGG pathway enrichment terms included 'cell cycle', 'p53 signaling pathway', 'Notch signaling pathway', 'β-alanine metabolism', 'glutathione metabolism', 'oxidative phosphorylation', 'arginine and proline metabolism', 'glyoxylate and dicarboxylate metabolism', 'insulin secretion' and 'homologous recombination' (Fig. 4).

Verification of the expression levels of MMDELs using RT-qPCR. To minimize selection bias, the expression levels of the six randomly selected MMDELs were verified using RT-qPCR. As presented in Fig. 5, the expression levels of these six MMDELs were in accordance with the results obtained using high-throughput RNA-seq. The expression levels of ENST00000621248, NONHSAT175141.1 and ENST00000530490 were significantly downregulated in the MM and HG groups compared with those of the LG group (P<0.05). However, the expression levels of ENST00000537869, ENST00000603538 and NONHSAT180590.1 were significantly increased in the MM and HG groups compared with those of the LG group (P<0.05). The expression levels of the six selected lncRNAs did not differ significantly between the MM and HG groups (P>0.05), indicating that the results of RNA-seq analysis were reliable.

Discussion

Various vascular complications, such as nephropathy, retinopathy and atherosclerosis, are responsible for the decreased quality of life and increased mortality in patients with diabetes. Increased levels of inflammation, non-enzymatic glycation of proteins and oxidative stress are common characteristics of the majority of complications observed in patients with diabetes. At present, MM is considered a major obstacle to implementing effective control of diabetes-related

Table II. Top 10 up-MMDELs and top 10 down-MMDELs with the highest node degree score.

A, HG vs. LG

lncRNA ID	Degree	Type	Locus	Fold change	P-value	Up- or downregulated
NONHSAT107810.2	210	Bidirectional	chr6	2.56318202	0.003	UP
NONHSAT180590.1	186	Exonic_sense	chr19	3.56619419	≤0.001	UP
ENST00000537869	180	Exonic_sense	chr11	3.33917148	≤0.001	UP
NONHSAT156713.1	148	Exonic_sense	chr10	3.18029669	≤0.001	UP
NONHSAT118785.2	125	Exonic_sense	chr7	6.98152837	≤0.001	UP
NONHSAT028252.2	96	Exonic_antisense	chr12	5.99732944	≤0.001	UP
NONHSAT135407.2	83	Intronic_sense	chr9	NA	0.006	UP
NONHSAT135581.2	80	Exonic_sense	chr9	2.69833263	0.001	UP
NONHSAT183181.1	75	Exonic_sense	chr2	3.28481839	0.008	UP
NONHSAT188701.1	74	Exonic_sense	chr20	13.06448443	≤0.001	UP
NONHSAT163874.1	240	Intronic_sense	chr12	0.17285088	≤0.001	DOWN
NONHSAT182446.1	209	Intergenic	chr2	0.14367777	0.016	DOWN
ENST00000623851	205	Intergenic	chr3	0.23109513	≤0.001	DOWN
NONHSAT194515.1	198	Intergenic	ch3	0.09350689	0.002	DOWN
NONHSAT215705.1	175	Exonic_sense	chr8	0.07170152	≤0.001	DOWN
NONHSAT155504.1	169	Intergenic	chr10	0.1565883	≤0.001	DOWN
NONHSAT175141.1	164	Intergenic	chr17	0.31294430	0.005	DOWN
NONHSAT200243.1	155	Exonic_sense	chr4	0.02487727	≤0.001	DOWN
NONHSAT156901.1	154	Intergenic	chr10	0.41563310	0.028	DOWN
ENST00000621248	151	Intergenic	chr12	0.21394491	≤0.001	DOWN

B, HG vs. MM

lncRNA ID	Node Degree	Type	Locus	Fold change	P-value	Up- or downregulated
NONHSAT107810.2	210	Bidirectional	chr6	1.25578160	0.453	NS
NONHSAT180590.1	186	Exonic_sense	chr19	1.40275545	0.292	NS
ENST00000537869	180	Exonic_sense	chr11	1.41459655	0.252	NS
NONHSAT156713.1	148	Exonic_sense	chr10	1.50549064	0.230	NS
NONHSAT118785.2	125	Exonic_sense	chr7	1.87617204	0.115	NS
NONHSAT028252.2	96	Exonic_antisense	chr12	1.62237440	0.136	NS
NONHSAT135407.2	83	Intronic_sense	chr9	1.06453167	1.000	NS
NONHSAT135581.2	80	Exonic_sense	chr9	1.22268316	0.544	NS
NONHSAT183181.1	75	Exonic_sense	chr2	1.36461675	0.351	NS
NONHSAT188701.1	74	Exonic_sense	chr20	0.82783165	0.674	NS
NONHSAT163874.1	240	Intronic_sense	chr12	0.47487294	0.156	NS
NONHSAT182446.1	209	Intergenic	chr2	0.65481627	1.000	NS
ENST00000623851	205	Intergenic	chr3	0.60246918	0.203	NS
NONHSAT194515.1	198	Intergenic	ch3	0.49615362	0.760	NS
NONHSAT215705.1	175	Exonic_sense	chr8	1.02467761	0.853	NS
NONHSAT155504.1	169	Intergenic	chr10	0.52492177	0.274	NS
NONHSAT175141.1	164	Intergenic	chr17	0.71489774	0.440	NS
NONHSAT200243.1	155	Exonic_sense	chr4	0.94930333	1.000	NS
NONHSAT156901.1	154	Intergenic	chr10	0.94316562	0.950	NS
ENST00000621248	151	Intergenic	chr12	0.51438924	0.064	NS

Table II. Continued.

C, LG vs. MM

lncRNA ID	Node Degree	Type	Locus	Fold change	P-value	Up- or downregulated
NONHSAT107810.2	210	Bidirectional	chr6	2.04110494	0.023	UP
NONHSAT180590.1	186	Exonic_sense	chr19	2.54227790	0.006	UP
ENST00000537869	180	Exonic_sense	chr11	2.36051154	0.008	UP
NONHSAT156713.1	148	Exonic_sense	chr10	2.11246527	0.021	UP
NONHSAT118785.2	125	Exonic_sense	chr7	3.72115576	≤0.001	UP
NONHSAT028252.2	96	Exonic_antisense	chr12	3.69663713	0.002	UP
NONHSAT135407.2	83	Intronic_sense	chr9	NA	0.009	UP
NONHSAT135581.2	80	Exonic_sense	chr9	2.20689441	0.018	UP
NONHSAT183181.1	75	Exonic_sense	chr2	2.40713620	0.046	UP
NONHSAT188701.1	74	Exonic_sense	chr20	15.78157158	≤0.001	UP
NONHSAT163874.1	240	Intronic_sense	chr12	0.36399395	0.022	DOWN
NONHSAT182446.1	209	Intergenic	chr2	0.21941693	0.042	DOWN
ENST00000623851	205	Intergenic	chr3	0.38358000	0.015	DOWN
NONHSAT194515.1	198	Intergenic	ch3	0.18846359	0.025	DOWN
NONHSAT215705.1	175	Exonic_sense	chr8	0.06997471	≤0.001	DOWN
NONHSAT155504.1	169	Intergenic	chr10	0.29830789	0.006	DOWN
NONHSAT175141.1	164	Intergenic	chr17	0.43774693	0.045	DOWN
NONHSAT200243.1	155	Exonic_sense	chr4	0.02620582	≤0.001	DOWN
NONHSAT156901.1	154	Intergenic	chr10	0.440678802	0.033	DOWN
ENST00000621248	151	Intergenic	chr12	0.41592027	0.022	DOWN

HG, high glucose; LG, low glucose; MM, metabolic memory; chr, chromosome; lncRNA, long non-coding RNA; MMDELs, MM-involved differentially expressed lncRNAs; NS, non-significant differential expression; NA, not applicable.

complications (35,36). Therefore, it is important to delineate the mechanisms underlying vascular complications and MM. In the present study, the expression profiles of lncRNAs were comprehensively analyzed in HUVECs from the LG, HG and MM groups, identifying a total of 308 up- and 157 downregulated MMDELs. GO analysis of the parental genes of these MMDELs suggested that the regulation of proteasomal ubiquitin-dependent catabolic process and DNA repair may participate in stress-caused vascular damage induced by exposure to HG in HUVECs. KEGG analysis indicated that in diabetic complications, the TGF-β and advanced glycation end products (AGE)-receptor for AGE (RAGE) signaling pathways may participate in MM-mediated pathogenic mechanisms induced by HG environments. Previous studies have demonstrated that AGE-modified proteins remain in the vessels, kidneys and hearts of patients with diabetes for extended periods of time, even after control of hyperglycemia is achieved in these patients. In addition, AGEs can induce oxidative stress and inflammation by interacting with RAGE receptors on the cellular surface. Therefore, the AGE-RAGE signaling pathway provides a clinical link between MM and diabetic complications (37-39). Additionally, the findings of the present study indicated that these pathways were enriched on the parental genes of MMDELs, which suggested that these lncRNAs may affect vascular endothelial cell function, cellular proliferation and apoptosis by altering the expression of parental genes.

In the present study, a bioinformatics analysis of target mRNAs was performed, which indicated that several DM-associated pathways, including cell cycle, p53 signaling and oxidative phosphorylation, may play a role in MM.

The present study indicated that 15 target genes were enriched in the cell cycle pathway, 14 of which had upregulated expression levels in MM compared with LG, including cyclin dependent kinase 1 (CDK1), Cyclin B1 (CCNB1) and CCNB2 (Table SI). This finding suggested that abnormal proliferation of vascular endothelial cells may lead to pathological angiogenesis, which is a crucial component of the pathological alterations observed in diabetic retinopathy (22). Furthermore, high levels of the CCNB1/CDK1 complex contribute to apoptosis by promoting cell cycle arrest at the mitotic prometaphase and induce the phosphorylation of antiapoptotic proteins, such as Mcl-1 and Bcl-xl, which can activate the subsequent intrinsic cell death pathway (40-42). CDK1 is an essential regulator of mitosis; therefore, CDK1 expression was predicted to be associated with 24 of the MMDELs identified in the present study. The present study indicated that 20 of these MMDELs had downregulated expression and were negatively correlated with CDK1 levels in MM compared with LG. The other four MMDELs, including lncRNA SNHG1 (ENST00000537869;

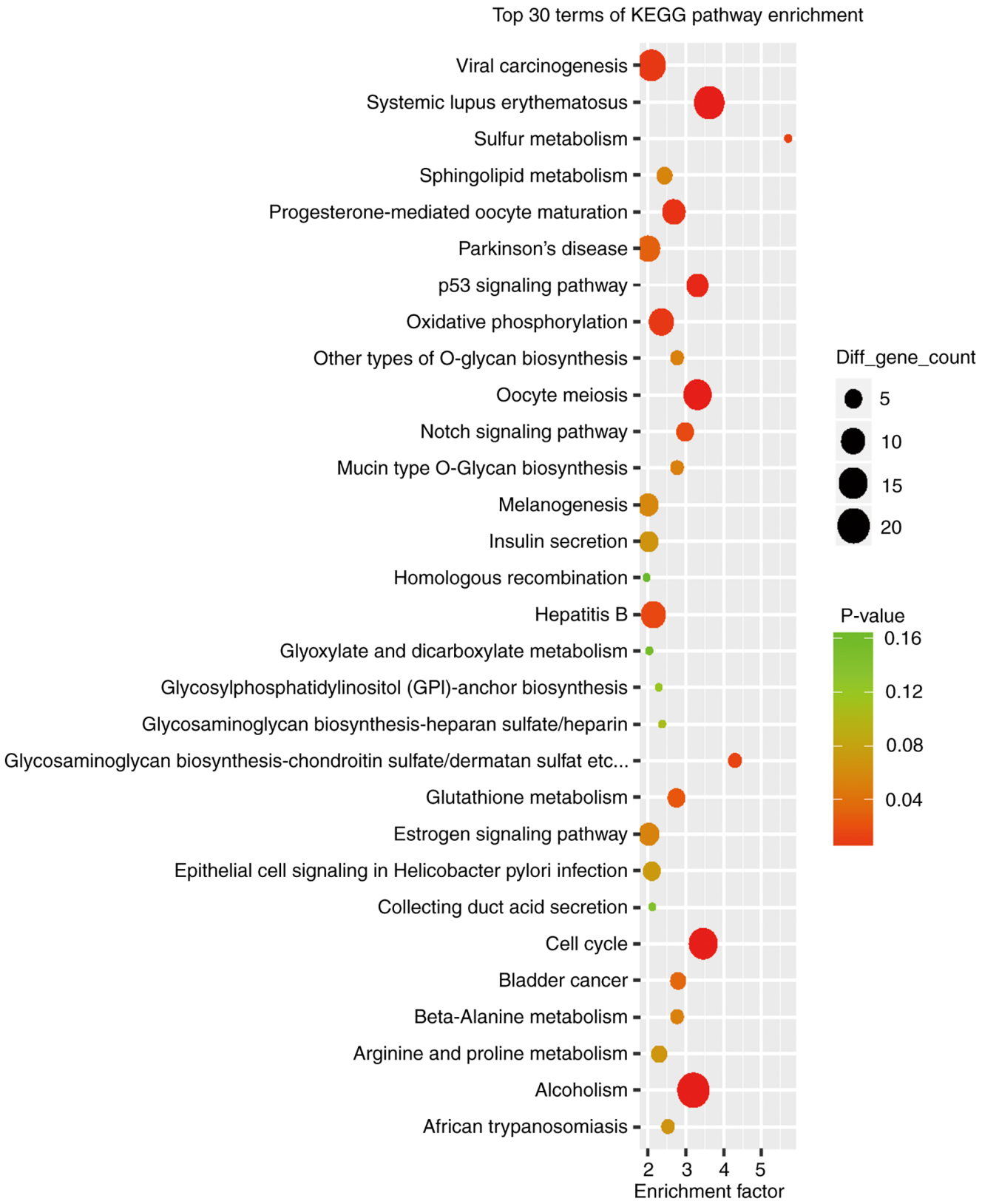

Figure 4. KEGG pathway enrichment analyses show the mRNA targets of metabolic memory-involved differentially expressed long non-coding RNAs. Top 30 KEGG pathway enriched terms. KEGG, Kyoto Encyclopedia of Genes and Genomes; Diff_gene_count, differential gene count.

node degree=180; up-MMDELs), had upregulated expression levels in MM compared with LG, a positive correlation with CDK1 levels and a strong positive correlation with the levels of CCNB1 and CCNB2.

The lncRNA SNHG1 is implicated in the progression of various cancers and is associated with a poor prognosis in patients with cancer. SNHG1 acts as a ceRNA to inhibit the expression of miR-140, thereby upregulating the expression

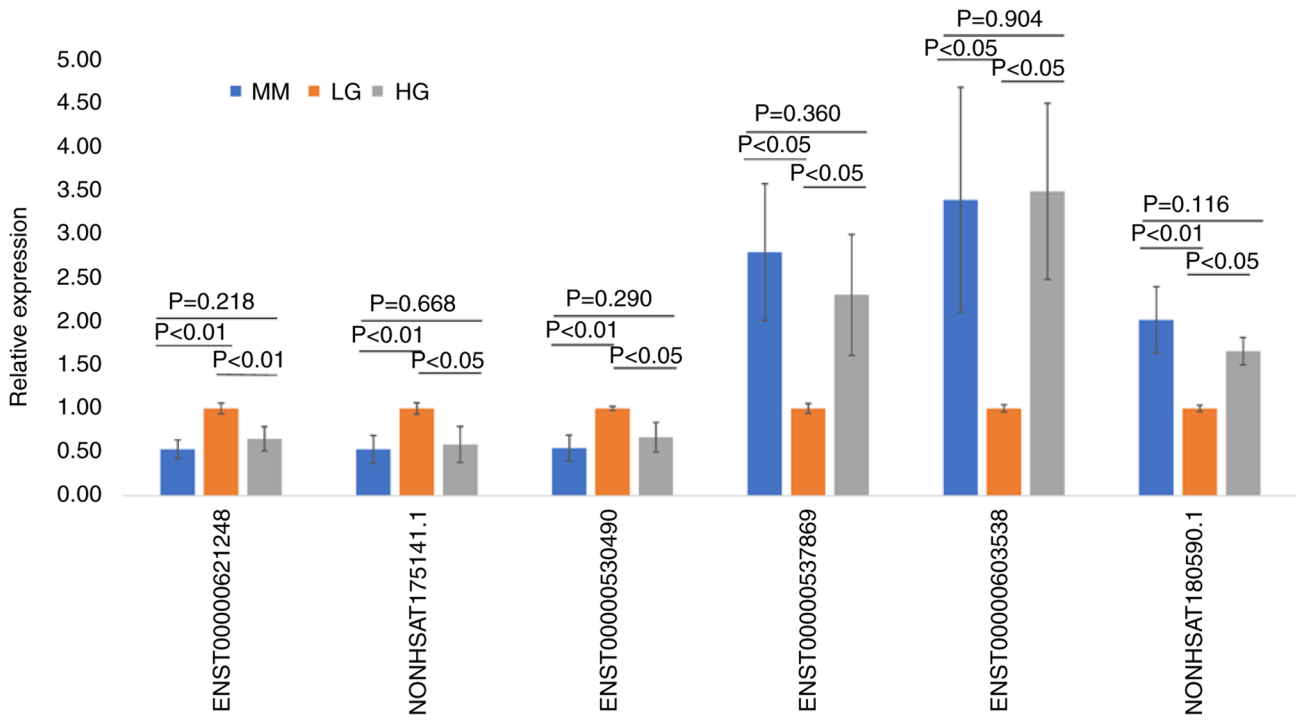

Figure 5. Verification of the MMDEL expression levels using reverse transcription-quantitative PCR. Expression levels of three MMDELs were increased and levels of the other three MMDELs were significantly decreased in the MM and HG groups compared with the expression levels of the LG group. HG, high glucose; LG, low glucose; MM, metabolic memory; MMDEL, MM-involved differentially expressed long non-coding RNAs.

of its downstream target, A disintegrin and metalloproteinase domain-containing protein 10, and promoting the proliferation and invasion of gastric cancer cells (43). Toll-like receptor 4 (TLR4) is a target of miR-140 (44). TLR4 expression can also be increased by SNHG1, which activates the NF-κB signaling pathway to regulate growth and tumorigenesis in cholangiocarcinoma tissues (44). SNHG1 promotes the expression of NUAK family SNF1-like kinase 1 by downregulating miR-145-5p expression, thereby promoting the invasion of nasopharyngeal carcinoma cells via the AKT signaling pathway (45). SNHG1 knockdown inhibits cancer cell migration and proliferation *in vitro* and *in vivo* (45,46). These findings suggest that upregulation of SNHG1 expression in HG environments may lead to proliferation abnormalities in vascular endothelial cells via mechanisms similar to those found in cancers. Specifically, interference with the expression of cell cycle-related regulatory molecules may occur via adsorption of specific miRNAs and the resultant upregulated expression of their target molecules.

The p53 signaling pathway, which mediates cell cycle arrest, cellular senescence and apoptosis, can be activated by various stressors including oxidative stress and DNA damage (47). The analysis of the present study indicated that eight target genes were enriched in this pathway and seven of these genes (Table SI), including CDK1, G2 and S phase-expressed-1 (GTSE1) and DNA damage-binding protein 2 (DDB2), had upregulated expression in MM compared with the LG group. GTSE1 leads to cell cycle arrest by inhibiting the expression of CDK1/CCNB. However, several previous studies have demonstrated that GTSE1 is overexpressed in several malignant tumors and is closely associated with tumor cell migration and invasiveness (48,49). Knockdown of GTSE1 expression suppresses the proliferation, migration and invasiveness of tumor cells (48). In the present study, 28 MMDELs were predicted to be correlated with GTSE1 expression; however, only four MMDELs, including lnc-FCN2-4:1 (NONHSAT135407.2; node degree=83; up-MMDELs), were upregulated and positively correlated with GTSE1 expression (Table SI and SII). Furthermore, lnc-FCN2-4:1 was also predicted to be correlated with CCNB1, CCNB2 and cell division cycle 20 expression. The expression of DDB2, which serves a key role in the repair of DNA (50), was associated with 15 of the MMDELs examined in the present study. Among these 15 MMDELs, eight had upregulated expression and were positively correlated with related lncRNAs, such as lncRNA SNHG1. The mechanism underlying the dysregulated expression of these lncRNAs, which were observed in HUVECs of the MM group in the present study, needs to be further explored in future studies.

Compared with the LG group, a total of 11 target genes were enriched in oxidative phosphorylation (OXPHOS) and five of these genes had upregulated expression in the MM group. Ubiquinol-cytochrome *c* reductase core protein 1 (UQCRC1), one of the five genes with upregulated expression, is a subunit of complex III of the respiratory chain in the mitochondria (51). UQCRC1 serves a fundamental role in normal mitochondrial function and cellular metabolism. Mutations and abnormal expression of UQCRC1 are associated with Parkinson's disease and multiple malignancies (52-54). In pancreatic ductal adenocarcinoma, increased expression of UQCRC1 mRNA promotes cellular proliferation by generating excessive levels of ATP and OXPHOS via the ATP/RTK/AKT pathway (53). In the present study, UQCRC1 expression was predicted to be positively associated with four MMDELs including lncRNA SNHG7 (NONHSAT135581.2;

node degree=80; up-MMDELs). SNHG7, which is highly expressed in certain neoplastic diseases, drives the occurrence and development of tumors by sponging miRNAs, such as miR-34a, miR-2682-5p and miR-449a, thereby promoting proliferation and suppressing apoptosis in cancer cells (55-57). SNHG7 is overexpressed in the areas surrounding the site of myocardial infarction. By acting as a ceRNA and targeting miR-34-5p expression, SNHG7 can promote cardiac fibrosis. Therefore, silencing SNHG7 expression can improve cardiac function (58). The present study indicated that the expression levels of MT-ND2, MT-ND3, MT-ND4L, MT-ATP8, MT-CYB and ATP6V1E1 were downregulated among 11 target genes in MM than LG group that were enriched in Oxidative phosphorylation (Table SI). The expression of MT-ND2, MT-ND3, MT-CYB and MT-ATP8 was positively associated with that of lncRNA XIST (NONHSAT137546.2; node degree=11; down-MMDELs) (Table SII). A previous study reported that knockdown of lncRNA XIST expression can inhibit proliferation, promote apoptosis, and even increase the production of reactive oxygen species (ROS) in non-small-cell lung cancer cells (59). It has been also demonstrated that mitochondrial dysfunction and fission can increase the levels of mitochondrial ROS (60,61). Excess accumulation of mitochondrial ROS in endothelial cells from diabetic patients results in cell death by damaging DNA, lipids and proteins, and leads to vasoconstriction caused by the decreased bioavailability of nitric oxide (62). These findings may partially explain the impairment of endothelial function in DM. Furthermore, based on the aforementioned findings and the results of the present study, it is proposed that the expression of OXPHOS-related mRNAs may be regulated by certain lncRNAs. These currently unknown and complex regulatory networks may be retained for extended periods of time in MM.

In summary, the present study analyzed the expression of MMDELs and the co-expression of mRNA networks in HUVECs subjected to conditions of LG, HG and induction of MM. The present study indicated that several MMDELs were abnormally expressed in experimentally-induced diabetic MM and may be involved in the regulation of mRNA expression through various mechanisms in MM-related pathways, which may play roles in the damage associated with long-term exposure to HG environments. The findings obtained in the present study contribute to improving the understanding of the molecular mechanisms underlying the pathology of MM. Further investigation into the functions of these lncRNAs may result in novel insights and treatments, which could help control MM in patients with diabetes.

Acknowledgements

The authors would like to acknowledge Mr. Qiang Fan (Shanghai Ao-Ji Biotechnology Co., Ltd., China) for technical assistance with RNA-seq experiments.

Funding

The present study was funded by the Key Program of Nature Science Foundation of Anhui Education Committee (grant no. KJ2019A0353), Key Project of Translational Medicine of Bengbu Medical College (grant no. BYTM2019039) and Key Project of Natural Science Foundation of Bengbu Medical College (grant no. 2020BYZD020).

Availability of data and materials

The datasets generated and/or analyzed during the current study are available in the National Center for Biotechnology Information, BioProject repository (accession no. PRJNA534362; https://www.ncbi.nlm.nih.gov/bioproject/PRJNA534362).

Authors' contributions

JinC and JiC contributed to acquisition of data for the work, wrote the draft of the paper and contributed to the literature review of the study. JiC performed the bioinformatics analysis. AH performed formal analysis and validation of sequencing data. LY and EX collected and analyzed RT-qPCR data. XP and AH contributed to formal bioinformatics analysis and the literature review. GJ conceived and designed the study. GJ and XP confirm the authenticity of all the raw data. All authors have read and approved the final manuscript.

Ethics approval and consent to participate

Ethics approval for the use of commercially purchased primary human cells was waived by the Ethics Committee of Bengbu Medical College (Bengbu, China).

Patient consent for publication

Not applicable.

Competing interests

The authors declare that they have no competing interests.

References

1. Jia G, Hill MA and Sowers JR: Diabetic cardiomyopathy: An update of mechanisms contributing to this clinical entity. Circ Res 122: 624-638, 2018.
2. Wong TY, Cheung CM, Larsen M, Sharma S and Simo R: Diabetic retinopathy. Nat Rev Dis Primers 2: 16012, 2016.
3. Shi Y and Vanhoutte PM: Macro- and microvascular endothelial dysfunction in diabetes. J Diabetes 9: 434-449, 2017.
4. Testa R, Bonfigli AR, Prattichizzo F, La Sala L, De Nigris V and Ceriello A: The 'Metabolic Memory' theory and the early treatment of hyperglycemia in prevention of diabetic complications. Nutrients 9: 437, 2017.
5. Giacco F and Brownlee M: Oxidative stress and diabetic complications. Circ Res 107: 1058-1070, 2010.
6. Chilelli NC, Burlina S and Lapolla A: AGEs, rather than hyperglycemia, are responsible for microvascular complications in diabetes: A 'glycoxidation-centric' point of view. Nutr Metab Cardiovasc Dis 23: 913-919, 2013.
7. Reddy MA, Zhang E and Natarajan R: Epigenetic mechanisms in diabetic complications and metabolic memory. Diabetologia 58: 443-455, 2015.
8. Reddy MA and Natarajan R: Epigenetic mechanisms in diabetic vascular complications. Cardiovasc Res 90: 421-429, 2011.
9. Thompson JA and Webb RC: Potential role of Toll-like receptors in programming of vascular dysfunction. Clin Sci (Lond) 125: 19-25, 2013.

10. Zhang HN, Xu QQ, Thakur A, Alfred MO, Chakraborty M, Ghosh A and Yu XB: Endothelial dysfunction in diabetes and hypertension: Role of microRNAs and long non-coding RNAs. Life Sci 213: 258-268, 2018.
11. Leung A, Amaram V and Natarajan R: Linking diabetic vascular complications with LncRNAs. Vascul Pharmacol 114: 139-144, 2019.
12. Biswas S, Thomas AA and Chakrabarti S: LncRNAs: Proverbial genomic 'Junk' or key epigenetic regulators during cardiac fibrosis in diabetes? Front Cardiovasc Med 5: 28, 2018.
13. Kung JT, Colognori D and Lee JT: Long noncoding RNAs: Past, present, and future. Genetics 193: 651-669, 2013.
14. Zhang X, Hong R, Chen W, Xu M and Wang L: The role of long noncoding RNA in major human disease. Bioorg Chem 92: 103214, 2019.
15. Singh KK, Mantella LE, Pan Y, Quan A, Sabongui S, Sandhu P, Teoh H, Al-Omran M and Verma S: A global profile of glucose-sensitive endothelial-expressed long non-coding RNAs. Can J Physiol Pharmacol 94: 1007-1014, 2016.
16. Xu E, Hu X, Li X, Jin G, Zhuang L, Wang Q and Pei X: Analysis of long non-coding RNA expression profiles in high-glucose treated vascular endothelial cells. BMC Endocr Disord 20: 107, 2020.
17. Leung A and Natarajan R: Long noncoding RNAs in diabetes and diabetic complications. Antioxid Redox Signal 29: 1064-1073, 2018.
18. Thomas AA, Feng B and Chakrabarti S: ANRIL: A regulator of VEGF in diabetic retinopathy. Invest Ophthalmol Vis Sci 58: 470-480, 2017.
19. Yan B, Yao J, Liu JY, Li XM, Wang XQ, Li YJ, Tao ZF, Song YC, Chen Q and Jiang Q: lncRNA-MIAT regulates microvascular dysfunction by functioning as a competing endogenous RNA. Circ Res 116: 1143-1156, 2015.
20. Liu JY, Yao J, Li XM, Song YC, Wang XQ, Li YJ, Yan B and Jiang Q: Pathogenic role of lncRNA-MALAT1 in endothelial cell dysfunction in diabetes mellitus. Cell Death Dis 5: e1506, 2014.
21. Qiu GZ, Tian W, Fu HT, Li CP and Liu B: Long noncoding RNA-MEG3 is involved in diabetes mellitus-related microvascular dysfunction. Biochem Biophys Res Commun 471: 135-141, 2016.
22. Zhang D, Qin H, Leng Y, Li X, Zhang L, Bai D, Meng Y and Wang J: LncRNA MEG3 overexpression inhibits the development of diabetic retinopathy by regulating TGF-β1 and VEGF. Exp Ther Med 16: 2337-2342, 2018.
23. Zhang E, Guo Q, Gao H, Xu R, Teng S and Wu Y: Metformin and resveratrol inhibited high glucose-induced metabolic memory of endothelial senescence through SIRT1/p300/p53/p21 pathway. PLoS One 10: e0143814, 2015.
24. Jin G, Wang Q, Pei X, Li X, Hu X, Xu E and Li M: mRNAs expression profiles of high glucose-induced memory in human umbilical vein endothelial cells. Diabetes Metab Syndr Obes 12: 1249-1261, 2019.
25. Kim D, Langmead B and Salzberg SL: HISAT: A fast spliced aligner with low memory requirements. Nat Methods 12: 357-360, 2015.
26. Pertea M, Kim D, Pertea GM, Leek JT and Salzberg SL: Transcript-level expression analysis of RNA-seq experiments with HISAT, StringTie and Ballgown. Nat Protoc 11: 1650-1667, 2016.
27. Pertea M, Pertea GM, Antonescu CM, Chang TC, Mendell JT and Salzberg SL: StringTie enables improved reconstruction of a transcriptome from RNA-seq reads. Nat Biotechnol 33: 290-295, 2015.
28. Nikolayeva O and Robinson M: edgeR for differential RNA-seq and ChIP-seq analysis: An application to stem cell biology. Methods Mol Biol 1150: 45-79, 2014.
29. Wang C, Li Q, Yang H, Gao C, Du Q, Zhang C, Zhu L and Li Q: MMP9, CXCR1, TLR6, and MPO participant in the progression of coronary artery disease. J Cell Physiol 235: 8283-8292, 2020.
30. Ashburner M, Ball C, Blake J, Botstein D, Butler H, Cherry JM, Davis AP, Dolinski K, Dwight SS, Eppig JT, *et al*: Gene ontology: Tool for the unification of biology. The gene ontology consortium. Nat Genet 25: 25-29, 2000.
31. Yu G, Wang L, Han Y and He Q: clusterProfiler: An R package for comparing biological themes among gene clusters. OMICS 16: 284-287, 2012.
32. Shannon P, Markiel A, Ozier O, Baliga NS, Wang JT, Ramage D, Amin N, Schwikowski B and Ideker T: Cytoscape: A software environment for integrated models of biomolecular interaction networks. Genome Res 13: 2498-2504, 2003.
33. Livak K and Schmittgen T: Analysis of relative gene expression data using real-time quantitative PCR and the 2(-Delta Delta C(T)) method. Methods 25: 402-408, 2001.
34. Knauss JL and Sun T: Regulatory mechanisms of long noncoding RNAs in vertebrate central nervous system development and function. Neuroscience 235: 200-214, 2013.
35. Singh R, Chandel S, Dey D, Ghosh A, Roy S, Ravichandiran V and Ghosh D: Epigenetic modification and therapeutic targets of diabetes mellitus. Biosci Rep 40: BSR20202160, 2020.
36. Berezin A: Metabolic memory phenomenon in diabetes mellitus: Achieving and perspectives. Diabetes Metab Syndr 10 (2 Suppl 1): S176-S183, 2016.
37. Yamagishi S, Fukami K and Matsui T: Crosstalk between advanced glycation end products (AGEs)-receptor RAGE axis and dipeptidyl peptidase-4-incretin system in diabetic vascular complications. Cardiovasc Diabetol 14: 2, 2015.
38. Yamagishi S and Matsui T: Role of receptor for advanced glycation end products (RAGE) in liver disease. Eur J Med Res 20: 15, 2015.
39. Koulis C, Watson AMD, Gray SP and Jandeleit-Dahm KA: Linking RAGE and Nox in diabetic micro- and macrovascular complications. Diabetes Metab 41: 272-281, 2015.
40. Choi HJ and Zhu BT: Upregulated cyclin B1/CDK1 mediates apoptosis following 2-methoxyestradiol-induced mitotic catastrophe: Role of Bcl-X_L phosphorylation. Steroids 150: 108381, 2019.
41. Choi HJ and Zhu BT: Role of cyclin B1/Cdc2 in mediating Bcl-XL phosphorylation and apoptotic cell death following nocodazole-induced mitotic arrest. Mol Carcinog 53: 125-137, 2014.
42. Harley ME, Allan LA, Sanderson HS and Clarke PR: Phosphorylation of Mcl-1 by CDK1-cyclin B1 initiates its Cdc20-dependent destruction during mitotic arrest. EMBO J 29: 2407-2420, 2010.
43. Guo W, Huang J, Lei P, Guo L and Li X: LncRNA SNHG1 promoted HGC-27 cell growth and migration via the miR-140/ADAM10 axis. Int J Biol Macromol 122: 817-823, 2019.
44. Li Z, Li X, Du X, Zhang H, Wu Z, Ren K and Han X: The Interaction Between lncRNA SNHG1 and miR-140 in Regulating Growth and Tumorigenesis via the TLR4/NF-κB pathway in Cholangiocarcinoma. Oncol Res 27: 663-672, 2019.
45. Lan X and Liu X: LncRNA SNHG1 functions as a ceRNA to antagonize the effect of miR-145a-5p on the down-regulation of NUAK1 in nasopharyngeal carcinoma cell. J Cell Mol Med 23: 2351-2361, 2019.
46. Yu Y, Zhang M, Wang N, Li Q, Yang J, Yan S, He X, Ji G and Miao L: Epigenetic silencing of tumor suppressor gene CDKN1A by oncogenic long non-coding RNA SNHG1 in cholangiocarcinoma. Cell Death Dis 9: 746, 2018.
47. Liu J, Zhang C, Wang J, Hu W and Feng Z: The regulation of ferroptosis by tumor suppressor p53 and its pathway. Int J Mol Sci 21: 8387, 2020.
48. Lai W, Zhu W, Li X, Han Y, Wang Y, Leng Q, Li M and Wen X: GTSE1 promotes prostate cancer cell proliferation via the SP1/FOXM1 signaling pathway. Lab Invest 101: 554-563, 2021.
49. Chen W, Wang H, Lu Y, Huang Y, Xuan Y, Li X, Guo T, Wang C, Lai D, Wu S, *et al*: GTSE1 promotes tumor growth and metastasis by attenuating of KLF4 expression in clear cell renal cell carcinoma. Lab Invest 102: 1011-1022, 2022.
50. Stoyanova T, Roy N, Kopanja D, Raychaudhuri P and Bagchi S: DDB2 (damaged-DNA binding protein 2) in nucleotide excision repair and DNA damage response. Cell Cycle 8: 4067-4071, 2009.
51. Hung Y, Huang K, Chen P, Li JL, Lu SH, Chang JC, Lin HY, Lo WC, Huang SY, Lee TT, *et al*: UQCRC1 engages cytochrome c for neuronal apoptotic cell death. Cell Rep 36: 109729, 2021.
52. Lin CH, Tsai PI, Lin HY, Hattori N, Funayama M, Jeon B, Sato K, Abe K, Mukai Y, Takahashi Y, *et al*: Mitochondrial UQCRC1 mutations cause autosomal dominant parkinsonism with polyneuropathy. Brain 143: 3352-3373, 2020.
53. Wang Q, Li M, Gan Y, Jiang S, Qiao J, Zhang W, Fan Y, Shen Y, Song Y, Meng Z, *et al*: Mitochondrial Protein UQCRC1 is Oncogenic and a potential therapeutic target for pancreatic cancer. Theranostics 10: 2141-2157, 2020.
54. Torricelli F, Saxena A, Nuamah R, Neat M, Harling L, Ng W, Spicer J, Ciarrocchi A and Bille A: Genomic analysis in short- and long-term patients with malignant pleura mesothelioma treated with palliative chemotherapy. Eur J Cancer 132: 104-111, 2020.
55. Sun X, Huang T, Liu Z, Sun M and Luo S: LncRNA SNHG7 contributes to tumorigenesis and progression in breast cancer by interacting with miR-34a through EMT initiation and the Notch-1 pathway. Eur J Pharmacol 856: 172407, 2019.

56. Wang W, Chen S, Song X, Gui J, Li Y and Li M: ELK1/lncRNA-SNHG7/miR-2682-5p feedback loop enhances bladder cancer cell growth. Life Sci 262: 118386, 2020.
57. Guo L, Lu J, Gao J, Li M, Wang H and Zhan X: The function of SNHG7/miR-449a/ACSL1 axis in thyroid cancer. J Cell Biochem 121: 4034-4042, 2020.
58. Wang J, Zhang S, Li X and Gong M: LncRNA SNHG7 promotes cardiac remodeling by upregulating ROCK1 via sponging miR-34-5p. Aging (Albany NY) 12: 10441-10456, 2020.
59. Liu J, Yao L, Zhang M, Jiang J, Yang M and Wang Y: Downregulation of LncRNA-XIST inhibited development of non-small cell lung cancer by activating miR-335/SOD2/ROS signal pathway mediated pyroptotic cell death. Aging (Albany NY) 11: 7830-7846, 2019.
60. Shenouda SM, Widlansky ME, Chen K, Xu G, Holbrook M, Tabit CE, Hamburg NM, Frame AA, Caiano TL, Kluge MA, *et al*: Altered mitochondrial dynamics contributes to endothelial dysfunction in diabetes mellitus. Circulation 124: 444-453, 2011.
61. Rovira-Llopis S, Banuls C, Diaz-Morales N, Hernandez-Mijares A, Rocha M and Victor VM: Mitochondrial dynamics in type 2 diabetes: Pathophysiological implications. Redox Biol 11: 637-645, 2017.
62. Pinti MV, Fink GK, Hathaway QA, Durr AJ, Kunovac A and Hollander JM: Mitochondrial dysfunction in type 2 diabetes mellitus: An organ-based analysis. Am J Physiol Endocrinol Metab 316: E268-E285, 2019.